Exploring the impact of Axion-Like Particles on keV–MeV Primordial Plasma

THEORY DEPARTMENT - CERN

Clara García Pérez, Universidad de Zaragoza

Supervisors: Miguel Escudero Abenza and Maksym Ovchynnikov

September 1, 2025

Abstract

This report focuses on the study of Axion-Like Particles and their impact in the early stages of the universe. A deep analysis is performed, taking into consideration the ALP photonic decay and its impact on the weak interconversion rates, and the ALP hadronic decay and its effect on the neutron-to-proton ratio. Constraints for ALPs parameters have been developed taking into consideration measurements from Big Bang Nucleosynthesis and Cosmic Microwave Background, specifically the abundance of Helium, Y_p, and N_{eff}. It has been observed that the ALPs decay into hadrons plays a crucial role in these constraints, as it has a great impact on the neutron-to-proton ratio, even if the initial abundance of ALPs is small. Additionally, different reheating temperatures, T_R, in which the ALPs could have been formed, have been studied. It has been observed that the constraints developed from the abundance of Helium, considering the hadronic decay, are less sensitive to the reheating temperature in comparison with the constraints from N_{eff}.

Contents

Introduction

The study of the early stages of the universe remains a major challenge in cosmology, and the Standard Model (SM) provides a theoretical framework to study it. Additionally, experiments help with the study of the beginning of the universe, going back to the Big Bang Nucleosynthesis (BBN) and Cosmic Microwave Background (CMB).

Before the BBN, there was a hot plasma of particles composed primarily of photons, electrons, and neutrinos, and nuclei couldn't be formed because of the high temperatures. However, as the universe expanded and the temperature dropped, the nuclei began to form during BBN. These abundances can be measured precisely, such as the abundance of Helium, Y_p, which provides an essential tool to study the universe. On the other hand, from the CMB the value of the effective number of neutrinos, N_{eff}, can be obtained, which is another key observable.

The most recent experiments provide the following values for the parameters mentioned previously: $N_{eff} = 2.81 \pm 0.12$ and $Y_p = 0.245 \pm 0.003$ [1]. There is some tension between the values predicted by the SM ($Y_p = 0.24709$ and $N_{eff} = 3.045$ [2]) and the measured ones, which motivates the exploration of new physics Beyond the Standard Model (BSM). In particular, this study focuses on the Axion-Like Particle (ALPs), which are hypothetical bosons and an extension of the Axion, a particle proposed initially as a solution for the Strong CP problem, and an excellent candidate for Dark Matter.

This report studies ALPs and their impact in the BBN, with the objective of studying the proton-neutron interconversion driven by the ALPs decay into hadrons as well as the effect of the ALPs' photonic decays on the weak conversion rates. Additionally, constraints on ALP parameters are derived from measurements of Y_p and N_{eff}. It is found that the decay of ALPs into hadrons provides stronger constraints, significantly affecting the neutron-proton ratio. Also, the study explores how different reheating temperatures, at which ALPs are considered to be produced, affect the different constraints, observing that the evolution of them is different for the case of Y_p, considering hadronic decay, and N_{eff}.

The report is organized as follows. Section 1 introduces the ALPs as well as how they are produced and how they decay, either into photons or hadrons. Section 2 shows the results from the simulations of the constraints of the parameters of the ALPs given by N_{eff} and Y_p. It is considered an arbitrary initial abundance of ALPs as well as a specific ALP production. Also, the results are shown for the evolution of constraints for different reheating temperatures. Finally, in Section 3, the conclusions of the report are shown.

1 Axion-Like Particles

Axion-Like Particles (ALPs) appear in many BSM theories. This report focuses on ALPs (that will be named a) coupled to photons, and their Lagrangian is written as follows: [3]

$$\mathcal{L} \simeq -\frac{g_a}{4} a F_{\mu\nu} \tilde{F}^{\mu\nu} \tag{1.1}$$

where F is the electromagnetic field tensor and g_a is the axion photon coupling. This coupling relates the mass (m_a) and the lifetime (τ_a) of the ALP.

$$\tau_a \equiv \frac{64\pi}{m_a^3 g_a^2} \tag{1.2}$$

Both the mass and the coupling of the ALP are treated as free parameters. Two decay channels of the ALPs will be considered: the decay into photons, which is the predominant one, and the decay into hadrons, which will have a smaller branching ratio, but its impact will be very significant.

1.1 ALPs production

For the production of ALPs, it is considered that at a temperature T_R (Reheating Temperature) there was no abundance of ALPs, taking a conservative perspective, and at this temperature the ALPs start to be produced. This is considering that before the BBN, some phenomena eventually led to the reheating of the universe at a temperature T_R, and the energy density of ALPs was negligible in comparison with the other species. After the reheating temperature, the ALPs are produced via two processes: the scattering of charged particles ($q^{\pm} + \gamma \rightleftharpoons q^{\pm} + a$) and the inverse decay ($\gamma + \gamma \rightleftharpoons a$) . From these two effects, the rate of production can be obtained from the formulas adapted from [4]

$$C_q(E,T) \simeq \sum_{i\in\{e,\mu,\ldots\}} \frac{g_a^2 \alpha}{16} \ln\Big(1 + \frac{(4E(m_i+E_i))^2}{m_\gamma(m_i^2 + (m_i+E_i)^2)}\Big) Q_i n_i(T) \tag{1.3}$$

$$C_\gamma(E,T) = \frac{m_a}{E\tau_a}\Big(1 + \frac{2T}{p_A}\ln\Big(\frac{1-e^{-(E+p_a)/2T}}{1-e^{-(E-p_a)/2T}}\Big)\Big) \tag{1.4}$$

Where $m_\gamma = eT\sqrt{g_q}/6$ is the plasmon mass in an electron-positron plasma [4] and $g_q^*(T)$ is the effective number of relativistic charged degrees of freedom, which is calculated in the following way

$$g_q^*(T) = \frac{\sum_{i\in\{e,\mu,\ldots\}} Q_i^2 n_i(T)}{\frac{3}{4}\zeta(3)T^3/\pi^2} \tag{1.5}$$

Where n_i is the number density of the charged fermions at a temperature T and Q_i is its charge in units of e. Only the fermions are considered, as they are the only charged particles participating in 1.3.

Once the rates are obtained, Boltzmann's equation can be used to calculate the abundance of ALPs at a time t_0, that in this study corresponds to T_0 = 20MeV when the ALP starts to decay, by integrating the following differential equation from T_R to T_0.

$$\frac{dY_a}{dt} = \Gamma_q(Y_a^{eq} - Y_a) \tag{1.6}$$

Where $Y_a = n_a/s$, being s the entropy density and n_a the number density of the ALPs, and $Y_a^{eq} = n_a^{eq}/s$ is the value at thermal equilibrium. An extended explanation of the calculation can be seen in Appendix A.

1.2 Axion-Like Particle decay

At a temperature $T = T_0$ the ALPs starts to decay efficiently into other particles. The most common decay channel of ALPs is into photons: $a \rightleftharpoons \gamma + \gamma$. However, ALPs can also decay into hadrons, with a smaller branching ratio. These processes affect N_{eff} and Y_p.

1.2.1 Photonic decays

When an ALP decays into photons, there is a transfer of energy to the electromagnetic plasma that can be calculated with the following coupled differential equations:

$$\begin{cases} \dfrac{dT_{\gamma/e}}{dt} = \dfrac{-3H\left(\rho_{\gamma/e} + P_{\gamma/e}\right) + \frac{\rho_a}{\tau_a} - \frac{\delta\rho_\nu}{\tau_\nu}}{\frac{\partial\rho_{\gamma/e}}{\partial T}} \\ \dfrac{dT_\nu}{dt} = \dfrac{-3H\left(\rho_\nu + P_\nu\right) + \frac{\delta\rho_\nu}{\tau_\nu}}{\frac{\partial\rho_\nu}{\partial T}} \\ \dfrac{d\rho_a}{dt} + 3H\rho_a = -\dfrac{\rho_a}{\tau_a} \end{cases} \tag{1.7}$$

The first two equations track the evolution of the temperature of the EM plasma and neutrinos in time, and the third one corresponds to the evolution of the energy density of the plasma in time. The term ρ_a/τ_a corresponds to the energy transfer from the ALPs to the plasma when they decay. Additionally, neutrinos decouple at $T \sim 1$MeV, causing them to stop sharing the same temperature as the plasma, leading to an exchange of energy between the plasma and the neutrinos. The term of exchange of energy, $\frac{\delta\rho_\nu}{\tau_\nu}$, has been obtained from [5] using $T_{\nu_e} = T_{\nu_\mu}$ and with $s_W = 0.223$.

$$\frac{\delta\rho_\nu(T_\nu, T_\gamma)}{\tau_\nu} = \frac{8G_F^2(1/2 + 2s_W^2 + 4s_W^4)}{\pi^5}[16(T_\gamma^9 - T_\nu^9) + 7T_\gamma^4 T_\nu^4(T_\gamma - T_\nu)] \tag{1.8}$$

For the expressions of energy density and pressure, the following expressions have been used, assuming Fermi-Dirac or Bose-Einstein distributions for fermions and bosons, respectively.

$$\rho_i = g_i \int \frac{d^3p}{(2\pi)^3} E f(E) \qquad f(E) = \frac{1}{e^{E/T} \pm 1} \qquad E = \sqrt{m^2 + p^2} \tag{1.9}$$

$$\rho_\gamma = \frac{\pi^2}{15} T_\gamma^4 \qquad\qquad \rho_\nu = 3\frac{7}{8}\frac{\pi^2}{15} T_\nu^4 \tag{1.10}$$

$$P = g_i \int \frac{d^3p}{(2\pi)^3} f_i(E) \frac{p^2}{3E} \tag{1.11}$$

By solving numerically the differential equations from 1.7, the values for the temperature of the plasma, temperature of the neutrinos, and energy density of the ALPs are obtained. The initial energy of the ALP is given by $\rho_a(t_0) = m_a \cdot n_a(t_0)$, as we are considering a non-relativistic particle. This can be considered a free parameter, or calculated as explained in Section 1.1. The change of temperatures produced by the presence of ALPs will have a direct effect on the value of N_{eff}, as its formula is

$$N_{eff} = 3\left(\frac{11}{4}\right)^{1/3}\left(\frac{T_\nu}{T_{\gamma/e}}\right)^4 \tag{1.12}$$

In Figure 1, it can be observed how the ALPs with different parameters affect the ratio of temperatures of the EM plasma and neutrinos, making a big impact on the observables.

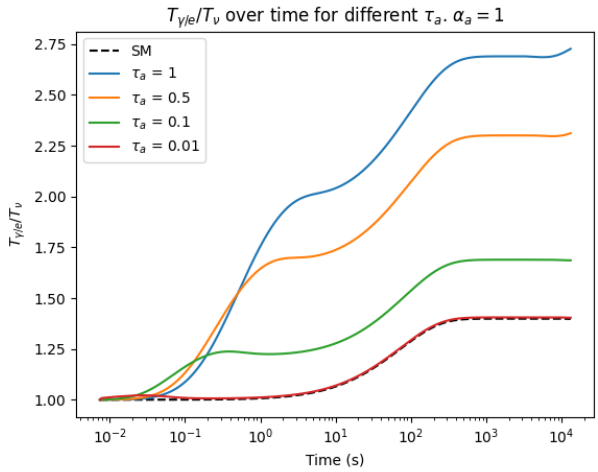

Figure 1: Evolution of $T_{\gamma/e}/T_\nu$ in time considering ALPs with $\alpha_a = \rho_a/\rho_{SM}(T_0) = 1$ and different lifetimes.

Once the temperatures have been obtained, the reactions of neutrons and protons must be studied. One relevant magnitude for this study is the proportion of neutrons X_n defined as:

$$X_n = \frac{n_n}{n_n + n_p} \tag{1.13}$$

The neutrons and protons are involved with leptons in the following reactions, changing the value of X_n.

$$n \leftrightarrow p + e^- + \bar{\nu}_e$$
$$p + e^- \leftrightarrow n + \nu_e$$
$$p + \nu_e \leftrightarrow n + e^+$$

The evolution of X_n is given by the following differential equation.

$$\frac{dX_n}{dt} = \Gamma_{p\to n}(1 - X_n) - \Gamma_{n\to p}X_n \tag{1.14}$$

The rates account for the proton conversion into neutrons ($\Gamma_{p\to n}$) and the neutrons into protons ($\Gamma_{p\to n}$) by the previous reactions. As $\Gamma = \Gamma(T_{\gamma/e}, T_\nu)$, the alteration of the temperatures will directly affect the rates and consequently the values X_n.

1.2.2 Hadronic decays

In addition to the decay of an ALP into photons, if the ALP is massive enough, it can decay into hadrons (h). It must follow the condition $m_a \geq 2m_h$. The process by which it is formed is that the ALP can decay into a photon γ and a virtual photon $\gamma*$, which will decay into hadrons. Once the hadrons are formed, they interact with protons and neutrons: $h + n/p \to p/n + \gamma$. In particular, this study will be focused in the production of pions, which correspond to masses of

ALPs of: $m_a \simeq 290 - 900$MeV. Taking larger masses would involve considering the production of other particles such as Kaons.

Pions

Pions can interact efficiently with protons and neutrons

$$\pi^- + p \to n + \pi^0/\gamma$$

$$\pi^+ + n \to p + \pi^0$$

The cross-sections of these reactions are the following [6]:

$$\langle \sigma^{\pi^-}_{p\to n} v\rangle \approx 4.3 \cdot 10^{-23} F^{\pi}_c(T) m^3/s$$

$$\langle \sigma^{\pi^+}_{n\to p} v\rangle \approx \frac{\langle \sigma^{\pi^-}_{p\to n} v\rangle}{0.9 F^{\pi}_c(T)}$$

Where F^h_c is the Sommerfeld enhancement of the cross-section due to the presence of two oppositely charged particles. Additionally, the pion decay width must be considered:

$$\Gamma^{\pi^\pm}_{decay} \approx 3.8 \cdot 10^7 s^{-1} \tag{1.15}$$

In order to solve the evolution of X_n taking into account the effect produced by n_{π^+}, n_{π^-} and n_a, the following system of coupled differential equations has to be solved [6].

$$\begin{cases} \dfrac{dX_n}{dt} = \left(\Gamma_{p\to n} + n_{\pi^-}\langle \sigma^{\pi^-}_{p\to n} v\rangle\right)(1-X_n) - \left(\Gamma_{n\to p} + n_{\pi^+}\langle \sigma^{\pi^+}_{n\to p} v\rangle\right) X_n \\ \dfrac{dn_{\pi^-}}{dt} = n_a \dfrac{Br_{a\to\pi^-}}{\tau_a} - \Gamma^{\pi^-}_{dec} n_{\pi^-} - \langle \sigma^{\pi^-}_{p\to n} v\rangle (1-X_n) n_B n_{\pi^-} \\ \dfrac{dn_{\pi^+}}{dt} = n_a \dfrac{Br_{a\to\pi^+}}{\tau_a} - \Gamma^{\pi^+}_{dec} n_{\pi^+} - \langle \sigma^{\pi^+}_{n\to p} v\rangle X_n n_B n_{\pi^+} \end{cases} \tag{1.16}$$

Where n_B is the baryon number density, given by:

$$n_B(T) = n_\gamma(T) \times \eta_{\text{baryon-to-photon}}(T_{CMB}) \times (\frac{a(T_f)T_f}{a(T)T})^3 \tag{1.17}$$

$$n_\gamma(T) = \frac{2\zeta(3)}{\pi^2 T^3} \tag{1.18}$$

However, for times $(\Gamma^h_{decay})^{-1} \sim 10^{-8}s$, that are small in comparison to the times scales that we are working with, there is a dynamical equilibrium that allows us to obtain analytical expressions for $n_{\pi^\pm}$ instead of differential equations [6].

$$n_{\pi^-} = \frac{n_a \cdot Br_{a\to\pi^-}}{\tau_a(\Gamma^{\pi^-}_{decay}) + \langle \sigma^{\pi^-}_{p\to n} v\rangle (1-X_n) n_B} \tag{1.19}$$

$$n_{\pi^+} = \frac{n_a \cdot Br_{a\to\pi^+}}{\tau_a(\Gamma^{\pi^+}_{decay}) + \langle \sigma^{\pi^+}_{n\to p} v\rangle X_n n_B} \tag{1.20}$$

These expressions reduce 1.16 to a single differential equation:

$$\frac{dX_n}{dt} = \left(\Gamma_{p\to n} + n_{\pi^-}\langle\sigma^{\pi^-}_{p\to n}v\rangle\right)(1-X_n) - \left(\Gamma_{n\to p} + n_{\pi^+}\langle\sigma^{\pi^+}_{n\to p}v\rangle\right)X_n \tag{1.21}$$

Consequently, the expression 1.21 provides a solid way for calculating X_n considering the weak interconversion rates, that depends on the temperature of the plasma and neutrinos; and $n_{\pi^\pm}$, which, as expressed in 1.20 and 1.19, depends explicitly on the lifetime and abundance of the ALPs.

In Figure 2, it can be seen the effect of the ALP decay on the value of X_n, clearly showing the great impact of including hadronic decays. For high temperatures, the hadrons make $n/p \approx 1$, and then the value of X_n decreases, having a different final value from the SM. On the other hand, the impact of the ALPs without considering hadronic decays is more subtle.

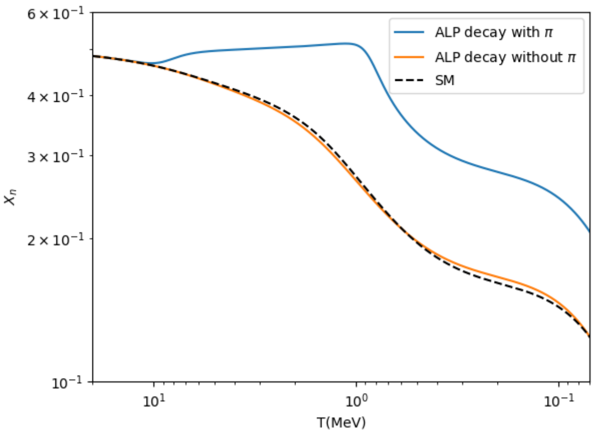

Figure 2: Evolution of X_n for different temperatures considering an ALP with these characteristics: $Br_{a\to\pi} = 0.001$, $m_a = 300$ MeV, $\tau_a = 0.1$, $\rho_a/\rho_{SM}(T_0) = 1$. The black line corresponds to the values of SM, the orange line corresponds to the value of X_n considering just the photonic decay of ALPs, and the blue line also considers the hadronic decays.

2 Results

The effect of the ALPs is given by their mass, their lifetime, and their initial abundance (which can be related to the two previous parameters). For these reasons, the space of parameters $\{m_a, \tau_a\}$ (or $\{m_a, \tau_a, \rho_a(0)\}$ if the initial energy density is taken as a free parameter without considering any relation) will be studied with the goal of analyzing the effect of the hadronic decay in different circumstances. Given that there are precise and accurate measurements of N_{eff} and Y_p: $N_{eff} = 2.81 \pm 0.12$ and $Y_p = 0.245 \pm 0.003$ [1], these values will be the reference for accepting or rejecting parameters as physically possible.

In the case of N_{eff}, a hypothesis test is performed at 95% confidence level, also the preferred or most likely region will be given by 1σ. In the case of Y_p, firstly, a theoretical uncertainty is considered, assuming the error for Y_p being ± 0.005. This way, the parameters will be physically possible if $\Delta Y_p/Y_p^{SM} < 2\%$, being Y_p^{SM} the abundance of Helium given by the code in the absence of ALPs. In this study, the value of Y_p is taken as $Y_p = 2 \cdot X_n(T = 0.078\text{MeV})$ and for N_{eff}, the temperatures of the EM plasma and neutrinos are taken at the end of the simulation at $T = 0.01$MeV.

2.1 Constrains depending on $\tau_a, m_a, \rho_a(T_0)$

First, ALP initial abundance is considered as a free parameter, without taking into account calculations of section 1.1. Therefore, there are three free parameters to consider $\{m_a, \tau_a, \rho_a(T_0)\}$. Figure 3 shows the constraints derived by the values of N_{eff} and Y_p for different masses. It can be observed that the great impact of the hadronic decay, in comparison with just considering photon decay (blue), results in bigger constraints. This is because the hadrons interact very efficiently with protons and neutrons, so only a small amount of ALPs can make a significant impact on the X_n ratio. The reason of this is because the cross section of the reactions mentioned above are much larger in comparison with the weak interconversion $\frac{\langle \sigma^{\pi}_{p\leftrightarrow n} v\rangle}{\langle \sigma^{Weak}_{p\leftrightarrow n} v\rangle} \simeq 10^6 \left(\frac{1\mathrm{MeV}}{T}\right)^2$[6].

Additionally, as the mass of the ALP increases, and as a consequence the branching ratio of hadron decay, the constraints on the ALP parameters are present for smaller initial abundances, giving orders of magnitude of difference in comparison with not considering them.

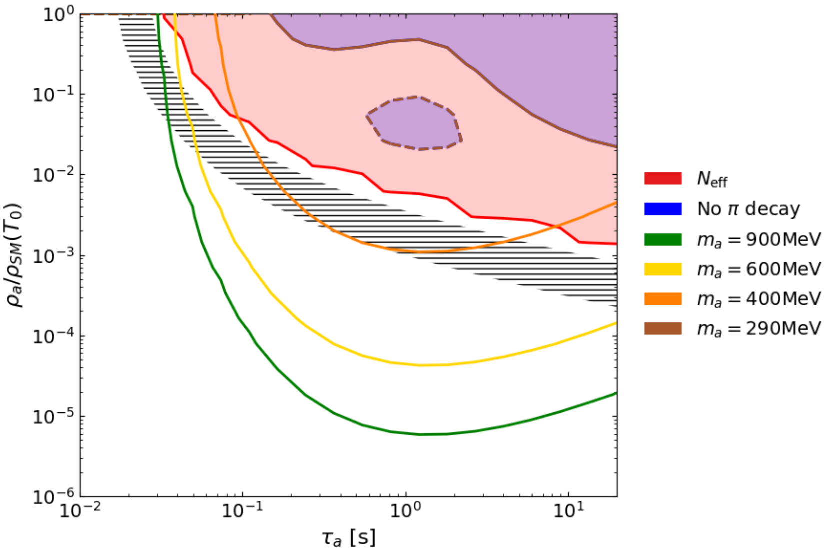

Figure 3: The solid lines separate the physically allowed regions (left) and the forbidden regions (right) on the parameter space, given by the comparison of the results obtained with the code and the measurements of [1]. The blue region corresponds to the forbidden region obtained with the value of Y_p without considering pion decay (if $\Delta Y_p/Y_p^{SM} > 0.02$, then it is forbidden). The red region corresponds to the forbidden region considering the value of N_{eff} with 95% of confidence. The black dashed region corresponds to the preferable region of the parameter space given by N_{eff} with 1σ. The different solid lines correspond to the constraints obtained with the value of Y_p considering the pion decay for masses of 900 MeV (green), 600 MeV (yellow), 400 MeV (orange), and 290 MeV (brown). Finally, the domain inside of the dashed lines corresponds to forbidden regions given by $\Delta Y_p/Y_p^{SM} < -0.02$.

2.2 Constrains depending on τ_a and m_a

For the next study, the initial abundance will be obtained with the procedure of section 1.1. Here, the temperature at which ALPs start to be produced will be considered very high $T_R = 10^{10}$MeV, and it will be integrated until $T_0 = 20$MeV. Consequently, now there are two free parameters: $\{m_a, \tau_a\}$.

It can be observed that the addition of hadron decay implies bigger constraints from Y_p, even exceeding the constraints from N_{eff} in some regions. Additionally, comparison with previous studies [3] shows good agreement.

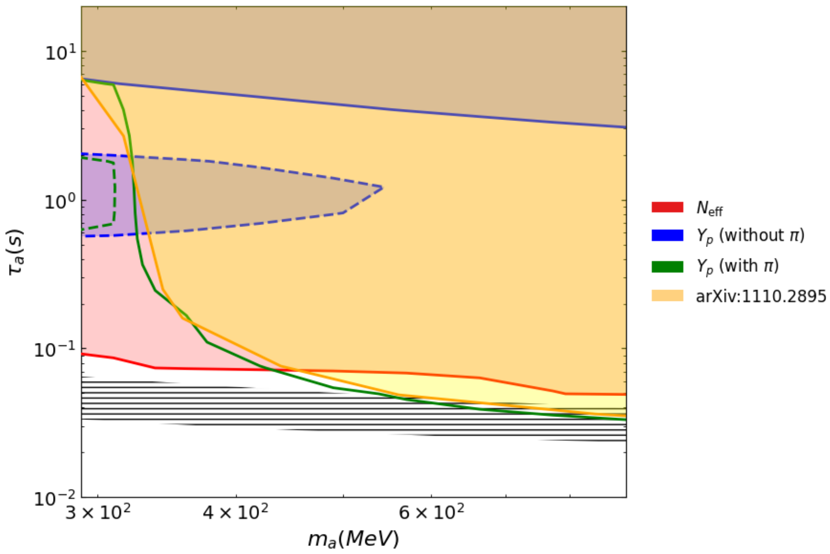

Figure 4: Constrains developed in the parameters of m_a and τ_a. The solid lines separate the physically allowed regions (left) and the forbidden regions (right) on the parameter space, given by the comparison of the results obtained with the code and the measurements of [1]. The blue region corresponds to the forbidden region obtained with the value of Y_p without considering pion decay (if $\Delta Y_p/Y_p^{SM} > 0.02$, then it is forbidden). The red region corresponds to the forbidden region considering the value of N_{eff} with 95% of confidence. The black dashed region corresponds to the preferable region of the parameter space given by N_{eff} with 1σ. The green line shows the constraints obtained from Y_p considering hadronic decays. The yellow region is the bounds obtained in the previous study [3].

2.3 Study of different reheating temperatures

In order to perform a deeper study, different reheating temperatures can also be considered. The early stages of the universe remain unknown to a great degree, so it is not possible to determine at which exact temperature the ALPs could have started to be formed. Consequently, it will be considered that at a temperature T_R there is no abundance of ALPs, and they begin to be produced at this temperature.

In the Figure, it can be observed how the different constraints change for different T_R. Considering the constraints derived from Y_p without considering the pion decay, it can be observed that as the reheating temperature decreases, this bound quickly disappears, as they are very sensitive to the initial abundance of ALPs. In the case of N_{eff}, the decrease of the constraints with T_R is very strong, observing a great effect when the temperature decreases. However, in the case of the constraints of Y_p considering the pion decay, they decrease more slowly than in the previous cases, showing strong constraints for low reheating temperatures (and consequently low initial abundances of ALPs). This is because, as was mentioned previously, just a small amount of pions can have a significant effect on the neutron-proton ratio. Also, by looking at the expression form [6] for the upper limit of the lifetime of a particle N that can decay into hadrons, given the upper bound on the Helium abundance

$$\tau_N \leq \frac{0.023(\frac{1.5\text{MeV}}{T_0^{min}})^2 s}{1 + 0.07\ln(\frac{P_{conv}}{0.1}\frac{Br_{N\to h}}{0.4}\frac{2n_{N,dec}}{3n_\gamma(T_{dec})}\cdot 24(\frac{a_{dec}T_{dec}}{a_0 T_0^{min}})^3)} \tag{2.1}$$

we find that the constraint will depend only logarithmically on the initial abundance of the particle N (in our study case, ALPs), which explains the slow decrease of these constraints.

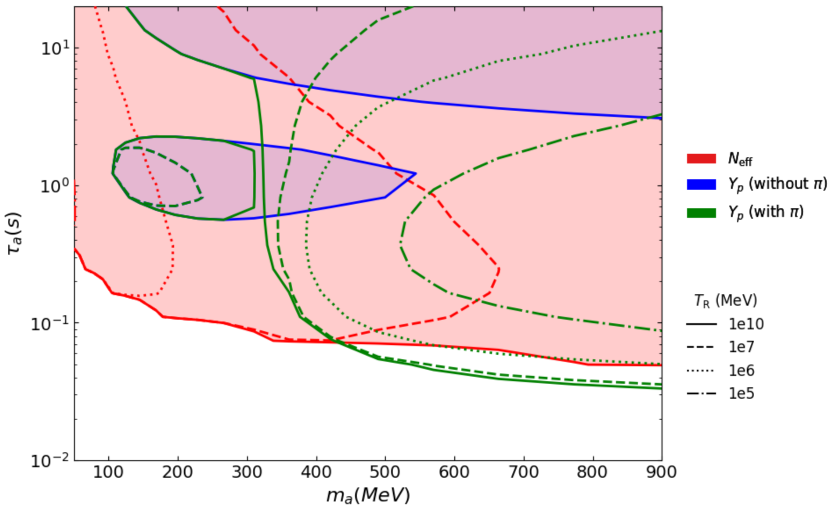

Figure 5: Constraints obtained from N_{eff} (red), Y_p without considering pion decay (blue), and considering it (green). The different dashed lines show the constraints for different reheating temperatures (solid: 10^{10} MeV, dashed; 10^7 MeV, points: 10^6 MeV, and lines and points: 10^5 MeV).

3 Conclusion

During this study, it has been studied the effect of ALP photonic and hadronic decays and its impact on Y_e and N_{eff} for developing constraints. It has been observed that the hadrons, specifically the pions, play a crucial role in neutron-proton interconversion, even with small initial quantities of ALPs and small branching ratios, as they interact very efficiently. As a consequence, it is extremely important to take them into consideration when developing constraints for the ALP parameters. Additionally, these constraints remain less sensitive to the reheating temperature, as they are less affected by the initial ALP abundance, while the constraints of N_{eff} and Y_e without considering pion decays change drastically.

As future steps, it would be relevant to increase the regions of parameters of ALPs, both in lifetime and in mass. However, it must be taken into consideration that for $m \gtrsim 1$ GeV, Kaons must also be considered. Also, constraints from other measures, such as D/H could be obtained and analyzed.

Additionally, the codes used for this project in python can be accessed via Github.

References

[1] E. Camphuis et al., *Spt-3g d1: cmb temperature and polarization power spectra and cosmology from 2019 and 2020 observations of the spt-3g main field*, 2025.

[2] P. F. de Salas and S. Pastor, "Relic neutrino decoupling with flavour oscillations revisited", Journal of Cosmology and Astroparticle Physics **2016**, 051 (2016).

[3] D. Cadamuro and J. Redondo, "Cosmological bounds on pseudo nambu-goldstone bosons", Journal of Cosmology and Astroparticle Physics **2012**, 032 (2012).

[4] P. F. Depta, M. Hufnagel, and K. Schmidt-Hoberg, "Robust cosmological constraints on axion-like particles", JCAP **05**, 009 (2020).

[5] M. Escudero, "Neutrino decoupling beyond the standard model: cmb constraints on the dark matter mass with a fast and precise neff evaluation", Journal of Cosmology and Astroparticle Physics **2019**, 007 (2019).

[6] A. Boyarsky et al., "Improved big bang nucleosynthesis constraints on heavy neutral leptons", Physical Review D **104**, `10.1103/physrevd.104.023517` (2021).

A Calculation of the ALP production rates

In order to obtain the production rates, expressions 1.3 and 1.4 are used. For obtaining Γ_q and Γ_γ we will need to integrate over the fermions and the ALPs in the following way, being f_{BE} and f_{FD} the Bose-Einstein and Fermi-Dirac distributions.

$$\Gamma_q(T) = \frac{\int_0^\infty \int_0^\infty \sum_{i\in\{e,\mu,...\}} C_q(E_i, E_a, T) p_i^2 f_{FD}(m_i, T)/(2\pi^2) p_a^2 f_{BE}(m_a, T)/(2\pi^2) dp_a dp_i}{\int_0^\infty p_a^2 f_{BE}(m_a, T)/(2\pi^2) dp_a} \tag{A.1}$$

$$\Gamma_\gamma(T) = \frac{\int_0^\infty C_\gamma(E, T) p_a^2 f_{BE}(m_a, T)/(2\pi^2) dp_a}{\int_0^\infty p_a^2 f_{BE}(m_a, T)/(2\pi^2) dp_a} \tag{A.2}$$

For calculating the value of C_q as well as the effective number of relativistic charged particles, $g_q^*(T)$, it is considered that for $T \geq 300$MeV both leptons e, μ, τ and quarks u, d, s, c, b, t existed. However for $T < 300$MeV only leptons will be considered because of the QCD transition, and quarks won't be part of this parameter. Also, the mesons, such as pions, won't be considered as they are bosons and don't participate in ALP production.

However, it must be taken in consideration that the calculation of the rate with the expression 1.3 and the one provided by [3] have some discrepancies. This last expression is the following

$$\Gamma_e = \frac{\alpha g_a^2}{12} T^3 \Big(\ln\Big(\frac{T^2}{m_\gamma^2}\Big) + 0.8194 \Big) \tag{A.3}$$

Expression A.3 is if we just considered electrons in the scattering process and for small ALP masses. When A.1 is calculated in this regime a misalignment of $\frac{\Gamma_q}{\Gamma_e} \approx 0.45$ is found. This differences should be treated as a future study case. However, for this study, the changes on the results using one expression or the other have been found to be small and qualitatively similar.

On the other hand, the expression 1.6 for calculating the evolution of Y_a comes from the following expressions:

$$\frac{dY_a}{dt} = \frac{d(n_a/s)}{dt} = \frac{1}{s}\frac{d(n_a)}{dt} - \frac{n_a}{s^2}\frac{ds}{dt}$$

As $s \propto a^{-3}$ the following expression can be obtained:

$$\frac{dY_a}{dt} = \frac{d(n_a/s)}{dt} = \frac{1}{s}\frac{d(n_a)}{dt} - \frac{n_a}{sa^{-3}} \cdot \frac{-3}{a^4}\frac{da}{dt} = \frac{1}{s}\frac{d(n_a)}{dt} + 3\frac{n_a}{s}\frac{1}{a}\frac{da}{dt}$$

We can express $H = \frac{1}{a}\frac{da}{dt}$ and $\frac{dn_a}{dt} = -3Hn_a + (\Gamma_q + \Gamma_\gamma)(n_a^{eq} - n_a)$. By substituting in the previous expression:

$$\frac{dY_a}{dt} = \frac{1}{s}(-3Hn_a + (\Gamma_q + \Gamma_\gamma)(n_a^{eq} - n_a)) + 3\frac{n_a}{s}H = (\Gamma_q + \Gamma_\gamma)(Y_a^{eq} - Y_a)$$